OVERVIEW OF RECENT RESULTS FROM HSX

D.T. ANDERSON, A. ABDOU, A.F. ALMAGRI, F.S.B. ANDERSON, D.L. BROWER[+], J. M. CANIK, C. DENG[+], W. GUTTENFELDER, C. LECHTE, K.M. LIKIN, H. LU, S. OH, P.H. PROBERT, J. RADDER, V. SAKAGUCHI, J. SCHMITT, J.N. TALMADGE, K. ZHAI

HSX Plasma Laboratory, University of Wisconsin-Madison
[+] *University of California-Los Angeles*

This paper is submitted as part of the special issue pertaining to the 15th International Stellarator Workshop

HSX Plasma Laboratory
1415 Engineering Drive
Madison, WI 53706

Email: talmadge@wisc.edu
Telephone: 608-262-2652
Fax number: 608-262-1267

Total number of pages: 18
Number of tables: 0
Number of figures: 8

OVERVIEW OF RECENT RESULTS FROM HSX

D.T. ANDERSON, A. ABDOU, A.F. ALMAGRI, F.S.B. ANDERSON, D.L. BROWER[+], J. M. CANIK, C. DENG[+], W. GUTTENFELDER, C. LECHTE, K.M. LIKIN, H. LU, S. OH, P.H. PROBERT, J. RADDER, V. SAKAGUCHI, J. SCHMITT, J.N. TALMADGE, K. ZHAI

HSX Plasma Laboratory, University of Wisconsin-Madison
[+] *University of California-Los Angeles*

Abstract

Recent results are summarized for the Helically Symmetric Experiment (HSX) which has the capability of running as a quasihelically symmetric stellarator (QHS) or as a more conventional, nonsymmetric stellarator. From X-ray measurements, we have demonstrated improved confinement of energetic particles. With central heating the density profiles in the quasisymmetric configuration are peaked, in contrast to the hollow or flat profiles when the symmetry is broken. The difference in profiles is attributed to the lowering of the neoclassical thermodiffusive flux when the symmetry is present. The central electron temperature is about 200 eV higher for the quasisymmetric configuration over the nonsymmetric case. The power deposition profiles are similar for the two cases implying that the neoclassical electron thermal conductivity is reduced with quasisymmetry. Related to the good confinement characteristics in the quasisymmetric mode of operation, fluctuations in density and magnetic field, consistent with that of a Global Alfven Eigenmode, are observed. While the neoclassical characteristics of the two configurations are very different, we have yet to find, under present operating conditions, any significant difference (other than the possible GAE mode) in turbulence characteristics or blob formation at the plasma edge.

1. Introduction

The Helically Symmetric Experiment (HSX) is the first operational quasisymmetric stellarator, with a helical direction of symmetry in the magnetic field strength. As a result of this symmetry, the neoclassical transport is reduced to the level of an axisymmetric device. The quasihelically symmetric (QHS) magnetic field, with a toroidal mode number of n = 4 and poloidal mode number of m=1, is produced with 48 non-planar modular coils. In addition to the main modular coils, there is a set of auxiliary coils that are used to raise and lower the transform and the magnetic well depth as well as the magnetic field spectrum and the resulting neoclassical transport. Two configurations in which the neoclassical transport is degraded with the addition of a toroidal mirror mode (n=4, m=0) are called the Standard Mirror (SM) and the Phase Shifted Mirror (PSM). On-axis Thomson scattering measurements can be made in PSM, while the axis is shifted about 1 cm inward for the SM configuration making on-axis Thomson measurements impossible. The two configurations differ by the phase of the toroidal mirror term. For most of the results reported here, plasmas are produced and heated with 40 kW of 2^{nd} harmonic electron cyclotron resonance heating at 28 GHz, and a magnetic field strength of 0.5 T. Previously we established that parallel viscous damping of flows is reduced with quasisymmetry.[1] In this paper we summarize recent experimental results obtained on HSX to further elucidate the differences between plasmas in quasisymmetric versus nonsymmetric configurations.

2. Confinement of Energetic Electrons

At an injected ECH power up to 130 kW, the central temperature in the QHS configuration was in excess of 1 keV at a density of 1.5×10^{12} cm^{-3}. Figure 1 shows the stored plasma energy measured by the diamagnetic loop as well as the integrated Thomson

density and temperature profiles versus the line average density for an injected power of 40 kW. It is seen that only at the higher plasma density does the kinetic energy coincide with the diamagnetic loop measurements. At low density, the difference in the stored energy is due to a large population of nonthermal electrons, which are very well confined in the QHS configuration. This is also confirmed by the large nonthermal emission observed by electron cyclotron emission (ECE) at low density.[2]

A CdZnTl detector is used to detect the hard X-ray flux for the QHS and SM configurations over a range of electron densities. Fig. 2a shows that the integrated flux is higher for the QHS configuration, especially at the lower densities. Calculations of particle orbits and energies in a microwave field using a Lorentz model indicate that the more efficient heating in the quasisymmetric configuration is due to the improved confinement. As seen in Fig. 2b, the integrated flux is higher for the QHS configuration at a fixed density of 4 $\times 10^{11}$ cm^{-3} , while the decay time for the signal in QHS (~ 7 msec) is longer than Mirror (~2.5 msec). This indicates that suprathermal electrons are confined for a longer time after the ECRH heating source is turned off compared to the Standard Mirror.

3. Particle and Heat Transport

Density profiles in stellarators during ECH are typically flat or hollow. In Wendelstein VII-AS for example, it has been shown that a peaked versus a flat density profile is a function of the balance between a thermodiffusive and an inward particle flux.[3] In other machines such as IMS[4] or Heliotron-E[5], the hollow profile is thought to be due to a convective flux driven by direct orbit losses. Calculations have shown that in large stellarators the thermodiffusive term may be so large as to drive hollow profiles that can cause serious density control problems.[6] In particular, it may be necessary in a stellarator

reactor to find a means by which to fuel the plasma core. We are interested in understanding how the density profile during ECH differs in quasisymmetric versus nonsymmetric plasmas.

Thomson Scattering is used to measure the electron temperature and density profiles. The system has 10 spatial channels with 2 cm resolution along a 20 cm laser beam path. The particle source has been measured using a suite of absolutely calibrated H_α detectors with a poloidal array covering the plasma cross-section at a fixed toroidal location, and several detectors distributed toroidally around the machine. This data from the H_α suite is interpreted from neutral gas modeling with the DEGAS code. [7]

Figure 3 shows a comparison of the electron density for the quasihelical configuration to the phase-shifted mirror. In the PSM case, the axis is shifted downward allowing a Thomson data point on both sides of the axis. With central ECH resonance and peaked temperature profiles, the density profile is also peaked for the QHS case. With the symmetry broken, the profile becomes flat to hollow in the mirror configuration. The flatness of the profile for the PSM is consistent with a larger thermodiffusive term. In contrast, the neoclassical thermodiffusive term is much smaller for the QHS configuration and is not large enough to hollow out the profile.

The central temperature in the QHS case is about 200 eV higher than for the PSM configuration: 450 eV compared to 250 eV for similar absorbed power profiles. This is shown in Figure 4. To study thermal transport, measurements of the absorbed power profile have been made using the Thomson scattering system. Measurements of the plasma density and temperature profiles were made in increments of 100 μs after the gyrotron turn-off for both the QHS and PSM configurations. In both cases the total absorbed power, based on the profile evolution, is 10 kW out of the 40 kW injected into the machine. The electron thermal diffusivity for the two cases is ~1 m^2/s in QHS, compared to ~ 3 m^2/s for PSM. The total

electron thermal conductivity is a sum of the neoclassical and anomalous contributions. The results indicate that reducing the neoclassical thermal conductivity for the quasisymmetric configuration has a clear effect on increasing the core temperature profile.

4. Fast Particle Driven Instability

Recent measurements on HSX have revealed the existence of coherent fluctuations in the electron density and magnetic field that suggest the presence of fast-particle driven instabilities. The mode has an m = 1 structure that peaks at r/a~0.5. When the ECRH power is turned-off, the fluctuations are observed to decay at a rate faster than both the soft x-ray signal and the energy confinement time. This suggests that fast electrons may be driving the instability. Figure 5 shows how the frequency of the mode decreases as the density increases, consistent with the dependence of a Global Alfven Eigenmode:

$$\omega_{GAE} \leq k_{//} v_A = \frac{(m\iota - n)}{R} \frac{B}{\sqrt{4\pi n_i m_i}} \tag{1}$$

The mode has also been observed in deuterium and helium discharges and shows an Alfvenic scaling with ion mass density. Some initial theoretical work, in collaboration with D. Spong of ORNL, further supports the possibility that this may be a GAE mode. Code runs from STELLGAP[8], using the HSX quasihelical equilibrium, predict a gap for the m=1, n=1 mode in the spectral region where the lower frequency fluctuations are experimentally observed.

A distinguishing feature of these fluctuations is that they are predominantly observed in the QHS configuration and may be a result of the superior confinement of energetic particles. The instability quickly decreases with the introduction of a toroidal mirror term and

is no longer observed when the perturbation reaches just 2%. The fast particle population is larger in the QHS configuration as compared to the 10% Mirror configuration, as evidenced by the soft and hard X-ray signals.

5. Edge Turbulence

Since advanced stellarators such as HSX have such low neoclassical transport, the role of anomalous transport becomes increasingly important as it could provide an upper bound to the global confinement time. Turbulent structures ("blobs") were investigated for various magnetic configurations and plasma conditions using a radially movable Langmuir probe that has 16 pins on a flux surface. A reference probe was positioned in close toroidal proximity, just inside the separatrix. With the help of cross correlation and conditional averaging[9], the time-dependent two-dimensional evolution of coherent structures is extracted.

Typically, on the low field side for the QHS configuration, turbulent structures in density and potential are seen moving poloidally in the direction of the E×B drift (see Fig. 6). A 2 to 2.5 cm blob, which is several times the drift radius ρ_s, is moving poloidally (upwards) in the direction of the E×B drift during the course of 4 μs. No marked radial movement of the structures was observed. Each density structure is accompanied by a potential structure of the same sign. The phase between density and potential, i.e. the spatial displacement of the potential blob with respect to the density blob, usually is small. This is consistent with drift wave dynamics. At higher densities, above 1×10^{12} cm^{-3} when the E×B drift reverses, the poloidal blob movement is also reversed. The blob characteristics did not vary much in the Mirror configuration as compared to QHS.

In HSX, the good and bad curvature regions rotate about the torus. Both can be accessed from the outboard side of the device at two different toroidal angles. Langmuir

probes are used to measure the poloidal and radial electric field (E_θ and E_r), the floating potential V_{float} and the density fluctuations $\tilde{n}$ at the plasma edge (r/a > 0.5). The turbulent particle transport Γ is determined from the density and potential fluctuations $\left\langle \tilde{n}\tilde{E}_\theta / B_\varphi \right\rangle$, where B_φ is the toroidal magnetic field. The two probes on the low and high field side used for these measurements are movable in the radial direction and have three tips aligned on a flux surface so that poloidal electric field, density and transport can be determined. We have investigated differences of transport and electric fields between the QHS configuration and the symmetry-breaking Mirror configurations. Edge density fluctuation levels are between 20 and 50%, which are consistent with mixing length estimates. The local wave number spectra of fluctuations yield mean poloidal wave numbers k_θ in the 0.5 to 2 cm^{-1} range. The drift radius ρ_s gives the scale for the smallest fluctuations. In HSX the value $k_\theta \rho_s \approx 0.1$ is similar to values observed on the edge of many toroidal fusion devices. Figure 8 shows that the edge turbulent flux is similar for both the QHS and Mirror configurations at a density of 1 x 10^{12} cm^{-3}. In both cases the directed particle flux is inward, but reverses direction at higher density. Radial correlations lengths, seen in Figure 8, as well as correlation times are also similar for the two configurations.

Summary

A number of different physics issues have been explored in a quasisymmetric stellarator and compared to configurations which have transport properties similar to those of conventional stellarators. Hard X-ray fluxes are larger in the QHS mode of operation, as well as having longer decay times after the gyrotron turn-off. Density profiles are more peaked in the QHS configuration, probably due to the lower thermodiffusive flux. Hotter central electron temperatures are achieved as well, indicative of a reduction of the neoclassical

electron thermal diffusivity in quasisymmetric plasmas. We have found a coherent fluctuation in density and magnetic field that may be a result of the good confinement of energetic trapped particles in HSX. Finally, initial measurements of coherent structures and edge turbulence for QHS and Mirror plasmas indicate little difference in anomalous transport. This may help explain why the density and temperature profiles in the outer regions of the plasma are roughly the same. In the near future, the magnetic field and the available heating power will both be doubled so that further comparisons of quasisymmetric and nonsymmetric plasmas will be made.

REFERENCES

[1] S.P. Gerhardt, J.N. Talmadge, J.M. Canik, and D.T. Anderson, Phys. Plasmas, 12 056116 (2005).

[2] K.M. Likin, A. Abdou, A.F. Almagri et al., Electron Cyclotron Heating by X-wave in the HSX stellarator, Joint Workshop on Electron Cyclotron Emission and Electron Cyclotron Heating (Proc. 13th Joint Workshop, May 2004), Nizhny Novgorod (Russia), 2005, 204-209.

[3] U. Stroth et al., Phys. Rev. Lett. 82 (1999) 928.

[4] J.N. Talmadge et al., Nucl. Fusion 29 (1989) 1806.

[5] H. Zushi, PPLK-R-27 (1988).

[6] Maassberg et al, Plasma Phys. Control. Fusion **41** 1135 (1999).

[7] D. Heifetz et. al., J. Comp. Phys. **46**, 309 (1982).

[8] D. A. Spong, Phys. Plasmas **10** 3217 (2003).

[9] C. Lechte, S. Niedner and U. Stroth, New J. Phys., **4**, 2002.

FIGURE CAPTIONS

Figure 1: Stored energy from diamagnetic loop and integrated Thomson profiles.

Figure 2(a) Hard X-ray counts versus density for the QHS and SM configurations. (b) Hard X-ray decay for QHS and SM.

Figure 3: Peaked density profiles in the QHS configuration compared to flat (or hollow) profiles in the PSM.

Figure 4: Profiles of electron temperature and absorbed power for QHS and PSM plasmas.

Figure 5: Wavelet spectrum showing frequency decreasing as density increases.

Figure 6: Results of the cross correlation for a QHS discharge at a line averaged density of 10^{12} cm^{-3}. A circular density structure (blob) moves poloidally upward, in the direction of the background E×B drift.

Figure 7: Turbulent fluxes for the QHS and SM plasmas are similar.

Figure 8: Radial correlation lengths for QHS and SM discharges are similar over a range of densities.

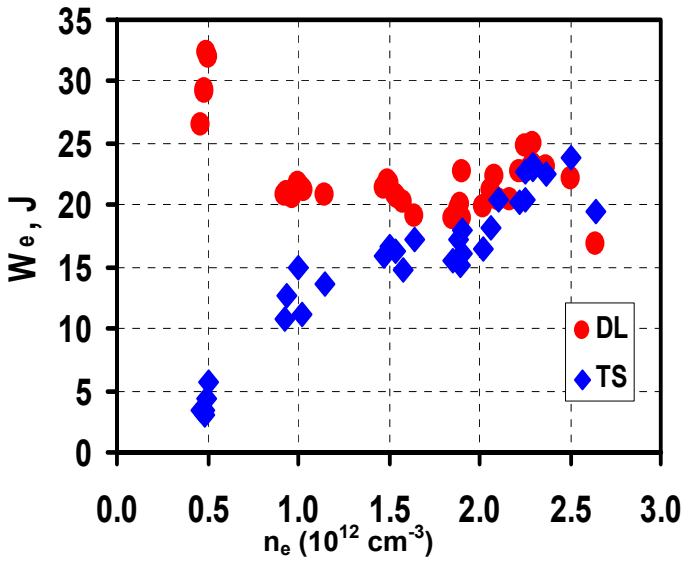

Figure 1

(a)

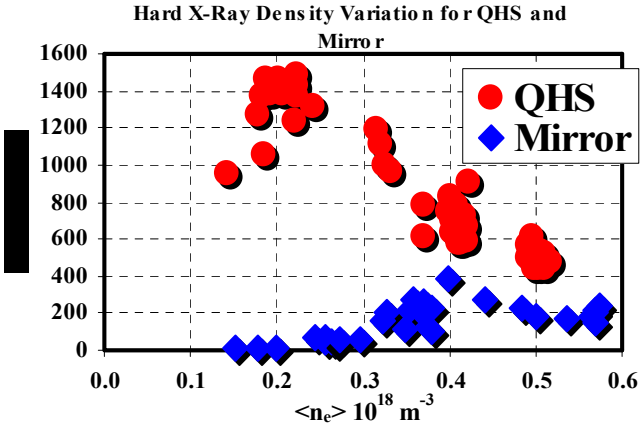
Hard X-Ray Density Variation for QHS and Mirror
1600
1400
1200
1000
800
600
400
200
0
0.0
0.1
0.2
0.3
0.4
0.5
0.6
<ne> 10^18 m^-3
QHS
Mirror

(b)

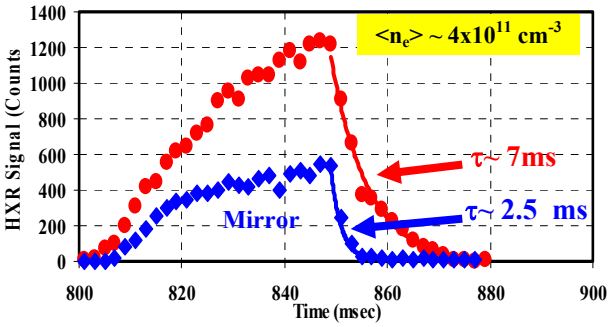
1400
1200
1000
800
600
400
200
0
HXR Signal (Counts
800
820
840
860
880
900
Time (msec)
<ne> ~ 4x10^11 cm^-3
τ~ 7ms
τ~ 2.5 ms
Mirror

Figure 2

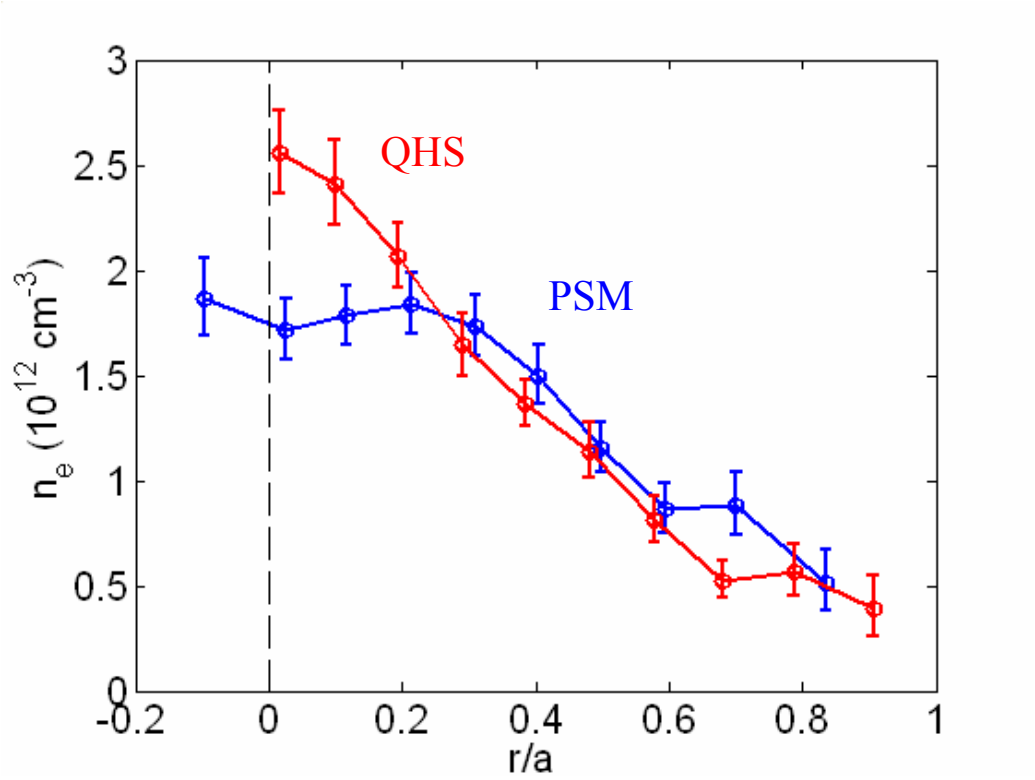

Figure 3

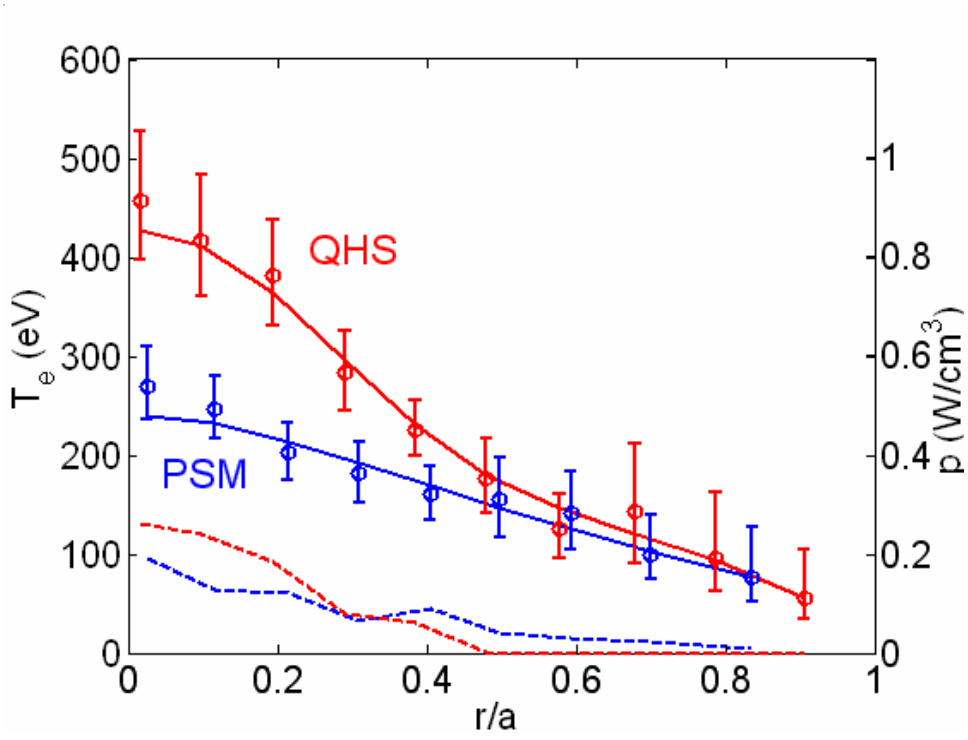
600
500
400
300
200
100
0
0
0.2
0.4
0.6
0.8
1
r/a
T_e (eV)
p (W/cm^3)
1
0.8
0.6
0.4
0.2
0
QHS
PSM

Figure 4

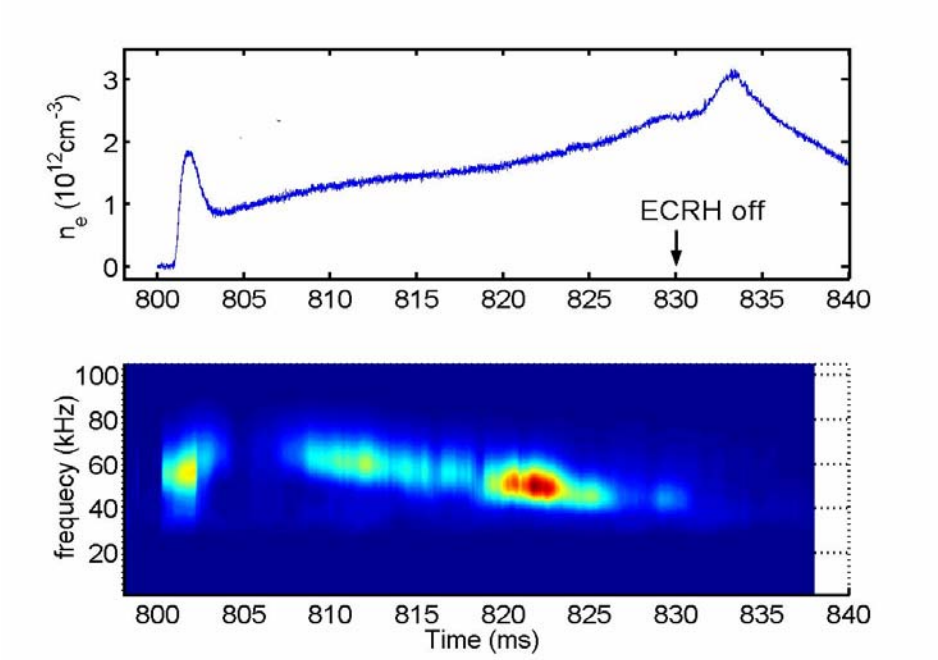
n_e (10^{12}cm^{-3})
3
2
1
0
ECRH off
800
805
810
815
820
825
830
835
840
frequecy (kHz)
100
80
60
40
20
Time (ms)

Figure 5

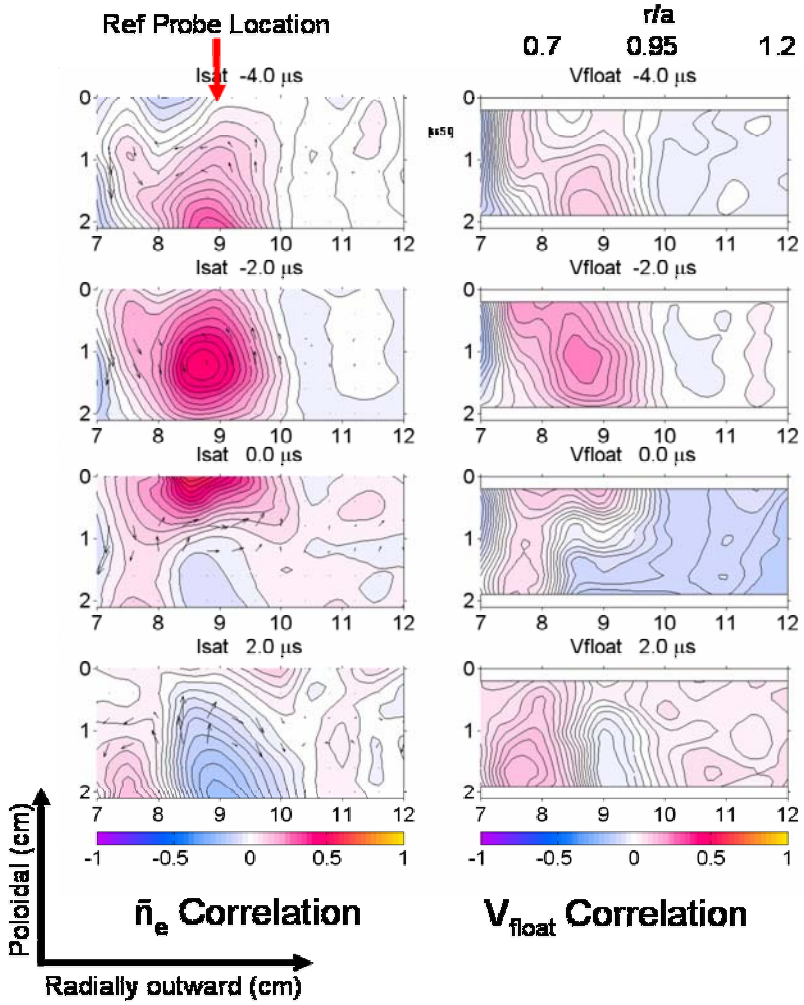
Ref Probe Location
r/a
0.7
0.95
1.2
Isat -4.0 μs
Vfloat -4.0 μs
Isat -2.0 μs
Vfloat -2.0 μs
Isat 0.0 μs
Vfloat 0.0 μs
Isat 2.0 μs
Vfloat 2.0 μs
Poloidal (cm)
Radially outward (cm)
ñe Correlation
Vfloat Correlation

Figure 6

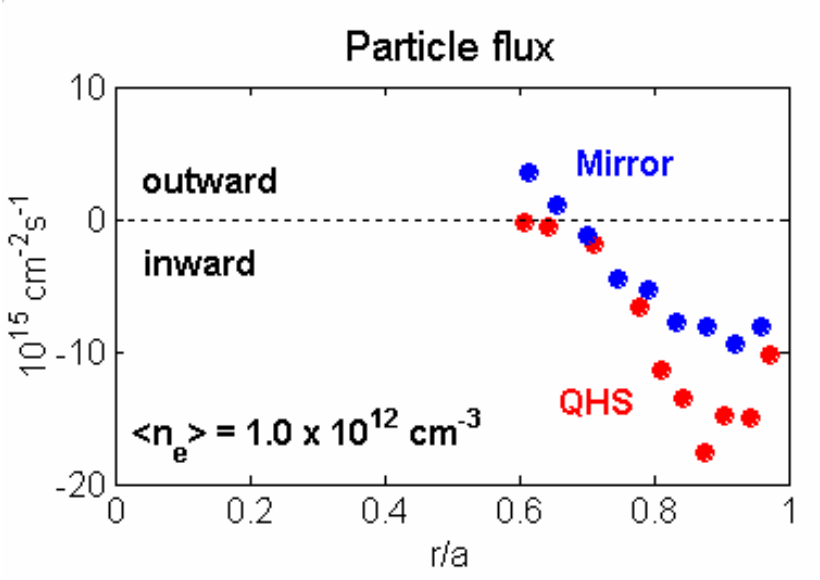
Particle flux
10
0
-10
-20
0
0.2
0.4
0.6
0.8
1
r/a
10^{15} cm^{-2}s^{-1}
outward
inward
Mirror
QHS
<n_e> = 1.0 x 10^{12} cm^{-3}

Figure 7

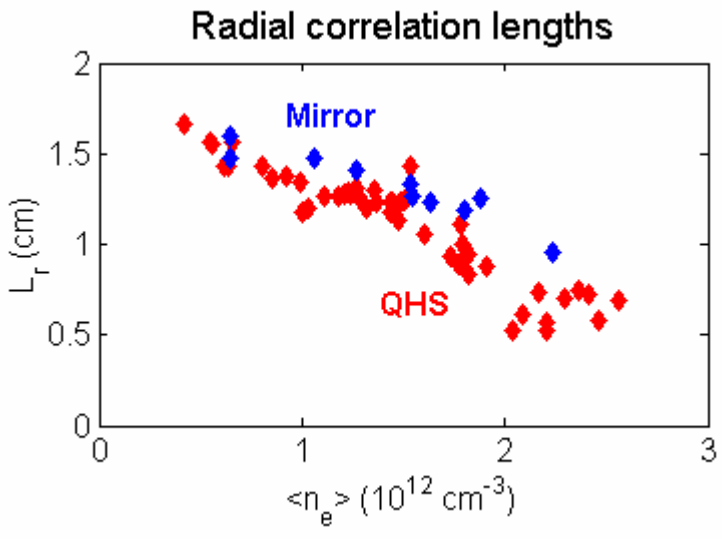
Radial correlation lengths
Mirror
QHS
L_r (cm)
$\langle n_e \rangle$ (10^{12} cm^{-3})
0
0.5
1
1.5
2
0
1
2
3

Figure 8